PROCEEDINGS, Fourteenth Workshop on Geothermal Reservoir Engineering
Stanford University, Stanford, California, January 24-26, 1989
SGP-TR-122

A Combined Heat Transfer and Quartz Dissolution/Deposition Model For a Hot Dry Rock Geothermal Reservoir

Bruce A. Robinson and John Pendergrass

Earth and Space Sciences Division
Los Alamos National Laboratory
Los Alamos, NM 87545

ABSTRACT

A kinetic model of silica transport has been coupled to a heat transfer model for a Hot Dry Rock (HDR) geothermal reservoir to examine the effect of silica rock-water interactions on fracture aperture and permeability. The model accounts for both the dissolution and deposition of silica. Zones of local dissolution and deposition were predicted, but their effect on aperture and permeability were fairly small for all cases studied. Initial rock temperature, reservoir size, and the ratio of rock surface area to fluid volume have the largest effect on the magnitude of silica mass transfered between the liquid and solid phases.

INTRODUCTION

Dissolution and deposition processes can have a large impact on plant operations and reservoir performance in both Hot Dry Rock (HDR) geothermal reservoirs and conventional geothermal systems undergoing fluid reinjection. For example, the deposition of dissolved silica in surface equipment and the injection wellbore is a well-known phenomenon which adversely affects plant operations (Cuellar, 1975, Bohlman et al., 1981, Rothbaum and Anderton, 1975, and Gudmundsson and Bott, 1979). Also, dissolution and deposition in the reservoir can affect the permeability by decreasing or increasing the flow path size (Rimstidt and Barnes, 1980, Horne, 1982, Robinson, 1982). For example, Horne (1982) reported that the problem of decreasing permeability near reinjection wells at the Hatchobaru and Otake geothermal fields in Japan may be caused by silica deposition.

Rock-water interactions in geothermal reservoirs are complex processes in which the mineralogy of the solid phase, chemical content of the fluid, and temperature all affect the behavior of the system. Nonetheless, simplified mathematical expressions have been proposed for certain minerals such as quartz. The behavior of quartz is among the most important in geothermal reservoirs because of the potential for large quantities of material to be dissolved or precipitated.

It is essential to combine a rock-water interaction model with a heat transfer model because of the strong dependence of temperature on quartz dissolution and deposition. Heat extraction from a HDR reservoir creates a thermal cooling front which is initially located near the injection wellbore and progresses with time toward the production wellbore. The produced fluids are reinjected without removal of dissolved silica. Thus, a driving force exists for deposition of silica on the cool rock near the injection wellbore, while a driving force exists for dissolution of the hot rock at distances beyond where the thermal effects of reinjection are felt. Since the temperature field within the reservoir is constantly changing due to heat extraction, the location in the reservoir where dissolution and deposition occur will change with time. The effect of these phenomena on permeability can be estimated by assuming that for flow through a fractured medium, dissolution or deposition of quartz results in a widening or narrowing of the fracture aperture. The magnitude of the aperture change is in turn related to the change in permeability through a relationship such as the cubic law.

In the present study, we present a model which couples a rate law for quartz dissolution and deposition to a HDR reservoir heat transfer model. The model is used to predict the rate of quartz dissolution and deposition in the reservoir and the effect of these rock-water interactions on the flow geometry and permeability within the reservoir.

MODEL DEVELOPMENT

Rock-Water Interaction Model. In a HDR geothermal reservoir, the produced fluid is reinjected after extracting the heat in a heat exchanger. The mass balance for dissolved silica in a closed-loop recirculating system is shown in Figure 1. Since some water loss to the host rock is always experienced, make-up fluid is added to the injection fluid to achieve a constant production flow rate. Therefore, the injection concentration C_{in} is

$$C_{in} = f_m C_m + (1-f_m)C_p \qquad (1)$$

where f_m is the make-up fluid flow fraction (typically 0.1-0.2), C_m is the make-up fluid

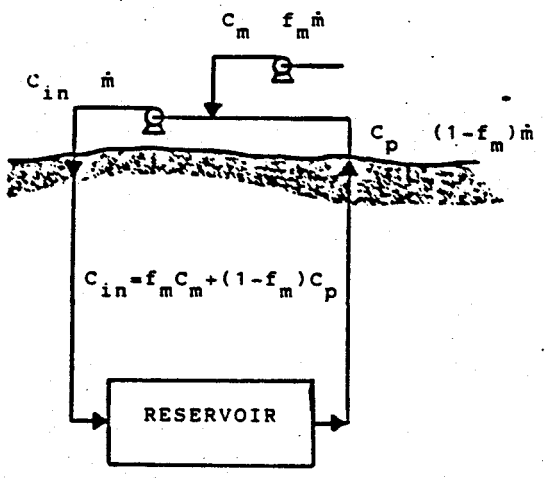

Figure 1. Mass balance on dissolved silica in a closed-loop HDR reservoir.

concentration, and C_p is the production fluid concentration. In practice, $C_m < C_p$, so that the production fluid is diluted with make-up fluid before reinjection.

The outlet concentration C_p is controlled by dissolution and deposition processes occurring in the reservoir. A commonly used rate law for quartz dissolution or deposition in a batch reactor is

$$\frac{dC}{dt} = ka^*(C^\infty - C) \qquad (2)$$

where t is time, a^* is the surface area to fluid volume ratio, k is the rate constant for quartz dissolution/deposition, and C^∞ is the saturation or equilibrium concentration of quartz in water. The temperature dependence of the equilibrium concentration was obtained by Rimstidt and Barnes (1980):

$$C^\infty = 6\times10^4 \times 10^{(1.881-2.028\times10^{-3}T-1560/T)} \qquad (3)$$

where T is the temperature in K and C^∞ has units of parts per million (ppm) as SiO_2.

The temperature dependence of dissolution rate constant k was determined by Robinson (1982) to be

$$k = 10^{(0.433-4090/T)} \qquad (4)$$

where the units of k are m/s. Finally, since fluid flow in HDR reservoirs occurs within fractures, a relationship for a^* is obtained by assuming the fracture can approximated by the parallel flat plate model:

$$a^* = \frac{2f_q}{w} \qquad (5)$$

In Eqn. (5), w is the mean fracture aperture and f_q is the fraction of quartz in the rock.

For modeling purposes, we assume that the fluid travels in plug flow between the wellbores, although in reality a distribution of solute residence times is always observed. For this parametric study, which is designed to evaluate the importance of dissolution and deposition processes, this assumption will not affect the results. For plug flow, dt = dx/u, and Eqn. (2) becomes

$$\frac{dC}{dx} = \frac{ka^*}{u}(C^\infty - C) \qquad (6)$$

To place this equation in terms of variables which can be measured directly, we make the substitution $u = \dot{m}L/V_f\rho_l$, where $\dot{m}$ is the fluid mass flow rate, L is the reservoir length, V_f is the reservoir fluid volume, and ρ_l is the density of water. Then, Eqn. (6) becomes

$$\frac{\partial C}{\partial x} = \frac{V_f\rho_l ka^*(C^\infty - C)}{\dot{m}L} \qquad (7)$$

This equation, coupled to the heat transfer model described below, is solved using finite difference techniques to obtain the steady state concentration as a function of position. Each time the temperature pattern is recalculated, a new steady state concentration profile is determined.

In addition to computing the concentration profile within the reservoir at various times, it is informative to examine the cumulative mass of silica dissolved from or deposited on the rock surfaces at each position in the reservoir. For a given time interval Δt, the mass of silica dissolved or deposited per unit length of reservoir m_q is given by

$$m_q = \frac{10^{-6}\rho_l \Delta t V_f ka^*(C^\infty - C)}{L} \qquad (8)$$

The quantity of silica dissolved or deposited can be related to the fractional change in the average fracture aperture by assuming a fracture flow geometry. Figure 2 shows the assumed geometry for both the rock-water interactions and the heat transfer model. Fluid flows along a series of parallel fractures of equal aperture w and fracture spacing S, with each fracture accepting the same flow rate. For the timestep Δt, the fractional aperture change Δw, which is equal to the volume change of quartz divided by the fluid volume, is

$$\Delta w = \frac{-Lm_q}{\rho_q V_f} = \frac{-LSm_q}{\rho_q w V_r} \qquad (9)$$

where ρ_q is the density of quartz and V_r is the total reservoir rock volume.

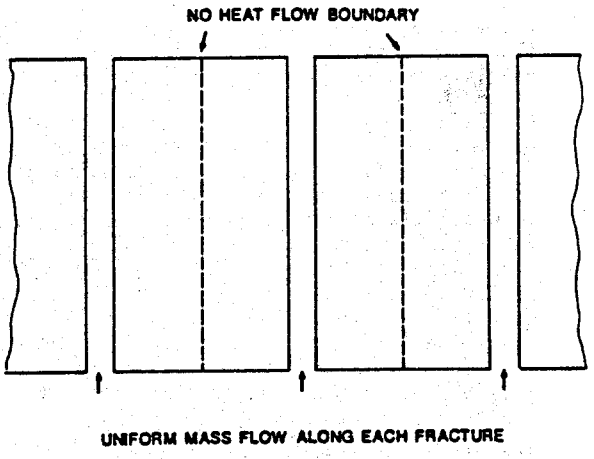

Figure 2. Fracture geometry for the heat transfer model.

Heat Transfer Model. The heat transfer model, based on the schematic diagram of Figure 2, was first treated analytically by Gringarten et al. (1975) for constant flow rate and inlet temperature. In the rock, the one-dimensional transient heat flow equation

$$\frac{\partial T}{\partial t} = \alpha \frac{\partial^2 T}{\partial x^2} \qquad (10)$$

is coupled to an energy balance equating convection in the fluid to conduction in the rock at the interface, which in terms of the variables used above, is:

$$\frac{\partial T}{\partial x} = \frac{LS\dot{m}c_f}{2k_r V_r} \frac{\partial T}{\partial y} \qquad (11)$$

In these equations, α is the rock thermal diffusivity, c_f is the fluid heat capacity, and k_r is the rock thermal conductivity. Due to symmetry, the boundary condition in the rock is a no-heat flow condition at the center of the rock block. To simulate time-varying flow rate and inlet temperature conditions, the model was solved by finite difference techniques. The model was verified by comparison to the solution of Gringarten et al. (1975) for constant flow rate and inlet temperature.

Figure 3 shows the internal temperature profiles at different times during heat extraction for different values of the fracture spacing S. For small S, the thermal wave passes through the reservoir as a sharp front. This extreme is sometimes referred to as volumetric heat extraction, since almost all of the heat within the rock volume is extracted. For large S, the front is more diffuse and significant temperature gradients remain within the rock blocks.

MODEL RESULTS

Figures 4a, b, and c demonstrate the behavior of the model for a typical set of reservoir

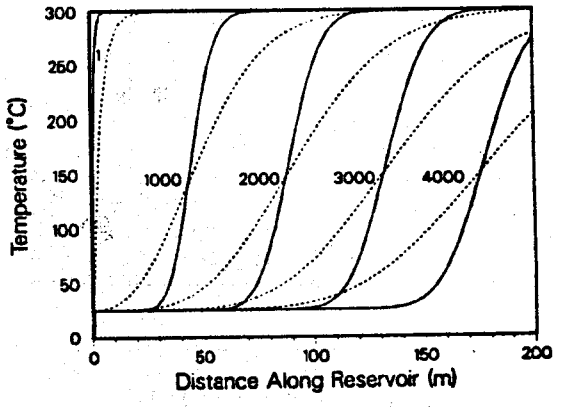

Figure 3. Temperature profiles at different times (in days) during long-term operation. Solid curves: S=2m, Dashed curves: S=10m.

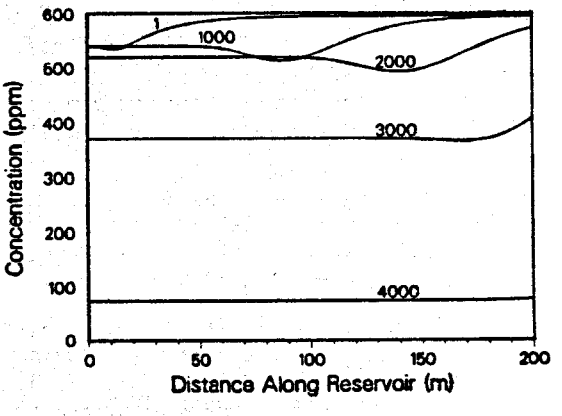

Figure 4a. Concentration profiles (time in days).

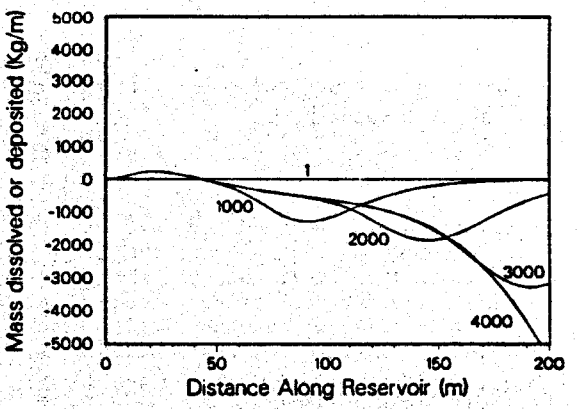

Figure 4b. Mass transfer profiles (time in days).

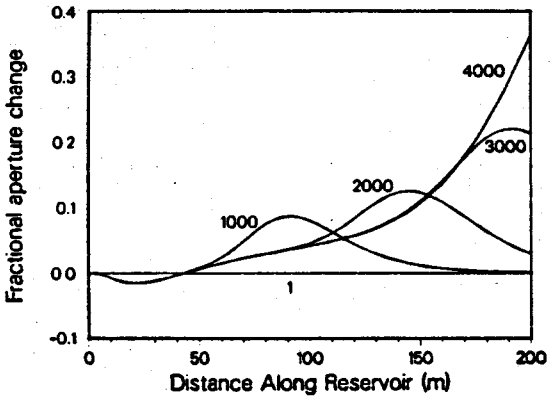

Figure 4c. Fractional aperture change profiles (time in days).

Figure 4. Internal profiles during long-term operation (time in days). T_r=300°C, S=10m, V_f=1.3x10^{8}m^3, $\dot{m}$=15kg/s, f_m=0.1, L=200m.

conditions (T_r=300°C, S=10m, V_f=1300m^3, $\dot{m}$=15kg/s, V_r=1.3x10^{8}m^3, f_m=0.1, and L=200m). Figure 4a shows the computed silica concentration profiles at different times during heat extraction. The fluid enters the reservoir supersaturated ($C>C^\infty$) due to cooling near the injection well, creating a driving force for deposition. The position of the thermal front dictates the location of the deposition. Although the largest driving force for deposition exists in the coolest region of the reservoir (near the inlet), the rate constant k is too small for significant deposition to occur. Deposition occurs in the transition region of rising temperature with distance, and the thermal wave is accompanied by a deposition front. When the fluid reaches the hotter portions of reservoir, deposition ceases and dissolution begins, resulting in an increase of dissolved silica, in this case to a maximum value of C^∞.

Dissolution and deposition result in residual silica depletion or buildup along the flowpath over time. Figure 4b shows the mass of silica dissolved or deposited per unit length of reservoir, and Figure 4c is the corresponding fractional aperture change. The amount of dissolution or deposition is controlled by the fraction of fresh make-up fluid in the injection fluid. For example, if f_m=1, the quantity of dissolved silica would be much greater, while if f_m=0 the net amount of silica removed from the reservoir would be zero. Deposition leaves a small zone of decreased aperture near the injection wellbore, but the magnitude of the change is small. Dissolution creates a larger zone of increased aperture and permeability which travels with the thermal wave. However, this zone is localized, rather than present across the entire reservoir. Therefore, the overall flow impedance, or pressure drop per unit flow rate, is unlikely to be much improved.

Figure 5 shows the effect of the mean fracture spacing S on the fractional aperture change after 2,000 days of operation. Small fracture spacings result in a sharp thermal front and more localized zone of dissolution and deposition. Thus, dissolution in a reservoir with larger fracture spacings results in a different residual pattern of the aperture profile. However, in all cases the effect on the permeability will be somewhat mitigated by the fact that significant portions of the reservoir remain at the initial aperture, unaffected by dissolution or deposition.

The effect of initial rock temperature on the dissolution and deposition processes is examined in Figure 6. Higher temperatures increase both the reaction rate and the magnitude of the changes possible from equilibrium considerations. Thus the changes in aperture are more pronounced at higher temperatures.

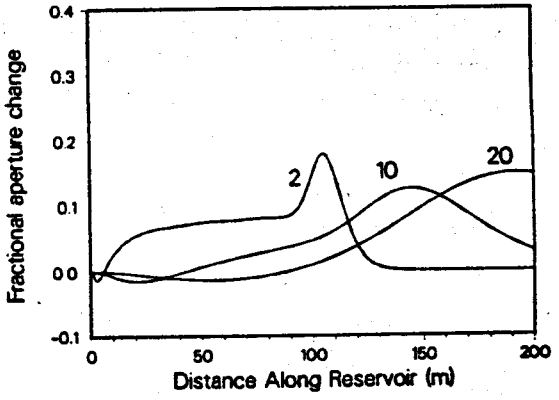

Figure 5. Fractional aperture change profiles for different fracture spacings S (after 2000 days).

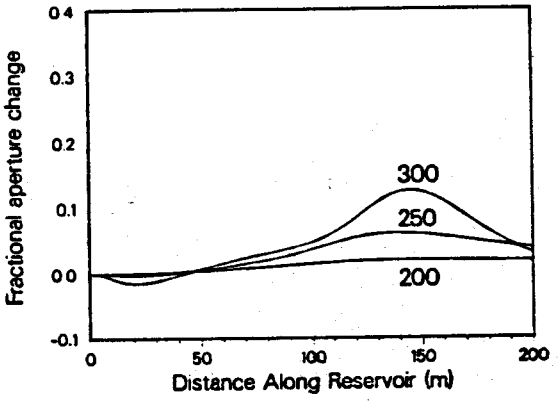

Figure 6. Fractional aperture change profiles for different initial rock temperatures T_r (after 2000 days).

DISCUSSION

Whenever a solution is undersaturated or supersaturated, the potential exists for dissolution or deposition. However, the amount of material exchanged between the solid and liquid phases depends on the kinetics of the reactions. In all cases examined, the deposition kinetics were such that a zone of decreased aperture was left near the injection wellbore. However, the effect on the crack width and permeability was found to be small. The zone of increased aperture and permeability due to dissolution was usually localized within a fraction of the reservoir length. Thus the effect on the overall flow impedance is also likely to be small.

In the silica mass balance model assumed (Eqn. (1)), it is assumed that heat is extracted without flashing the brine. In energy conversion schemes in which the brine is flashed, the reinjected liquid has a much higher concentration of all dissolved species, including silica. Thus, the potential exists for more severe deposition near the injection wellbore. One advantage of the binary cycle energy conversion schemes usually proposed for HDR reservoirs is that deposition problems are minimized by keeping the brine liquid.

When assessing the effect of rock-water interactions on permeability, we must recognize that other effects will occur simultaneously to either enhance or negate the effects of dissolution and deposition. First, thermal stress cracking of the rock is thought to occur near the injection well (Tester et al., 1986), increasing the permeability and competing with the effect of deposition. Also, pressures are highest near the injection wellbore, which, according to current theories of flow through fractured rocks, cause the fractures to dilate and the permeability to increase (Brown and Fehler, 1989). Finally, the effect of dissolution on the aperture and permeability will depend on the location of the quartz grains relative to the asperities upon which the fracture faces rest. In fact, if the asperities are largely quartz, dissolution would cause the fracture faces to collapse on each other, lowering the aperture and permeability. Clearly, when estimating the effect of rock-water interactions on the permeability of a HDR reservoir, these phenomena must be considered. However, they are beyond the scope of this study.

Another area in which further study is warranted is in the form of the rate law used to describe quartz dissolution and deposition. In the present study, a single rate equation with a common rate constant was assumed to model both dissolution and deposition. Although Rimstidt and Barnes (1980) claim that the reaction is reversible and Eqn. (2) is valid, some studies have stated that in the temperatures of interest for HDR reservoirs, the deposition of silica is controlled by amorphous silica rather than quartz (e.g. White et al., 1956). Others have noted the possibility of both homogeneous and heterogeneous nucleation mechanisms for silica precipitation (Gudmundsson and Bott, 1979). Finally, Makrides et al. (1978), and Marsh et al. (1975) examined the effect of pH on the reaction kinetics. However, other than the model of Rimstidt and Barnes (1980), no comprehensive model of quartz dissolution and silica deposition has been proposed which includes the temperature dependence of the reactions. Therefore, Eqn. (2) was used in the present study. Future work should incorporate more complex laws for quartz dissolution and deposition when they become available.

CONCLUSIONS

A quartz dissolution/deposition kinetic model has been coupled to a heat transfer model to examine the silica rock-water interactions occurring in a HDR geothermal reservoir. The temperature dependence of the reaction rates makes modeling of the temperature pattern within the reservoir essential. Near the injection well, where temperatures are lovest, the fluid is supersaturated with respect to dissolved silica, and a driving force exists for deposition. However, under all conditions studied, the computed deposition rate was insufficient to cause significant decreases in the fracture aperture near the injection well. Dissolution occurs in the hotter portions of the reservoir, but its effects are usually localized: only a fraction of the total flow system experiences an increase in fracture aperture. Thus, permeability enhancement due to dissolution will probably be small.

In future studies, these model results should be compared to the results of calculations of thermal stress cracking and pressure dependent dilation of joints to assess the relative importance of rock-water interactions. Furthermore, when available, rate laws incorporating the effect of pH and different silica phases such as amorphous silica should be coupled to the heat transfer model to refine the results presented here.

NOMENCLATURE

a^*	surface area to fluid volume ratio (m^{-1})
C	concentration (ppm)
c_f	heat capacity of the fluid (J/kg-K)
C_{in}	inlet silica concentration (ppm)
C_m	make-up fluid silica concentration (ppm)
C_p	production fluid silica concentration (ppm)
C^∞	equilibrium silica concentration (ppm)
f_m	make-up fluid flow fraction
f_q	fraction of quartz in the rock
k	reaction rate constant (m/s)
k_r	thermal conductivity of the rock (W/m-K)
L	reservoir length (m)
$\dot{m}$	fluid mass flow rate (kg/s)
m_q	mass of quartz dissolved or deposited per unit length of reservoir (Kg/m)
S	mean fracture spacing (m)

T	temperature (K)
T_r	initial rock temperature (K)
u	fluid velocity (m/s)
V_f	reservoir fluid volume (m^3)
V_r	reservoir rock volume (m^3)
w	mean fracture aperture (m)
x	flow path direction (m)
α	rock thermal diffusivity (m^2/s)
ρ_l	fluid density (kg/m^3)
ρ_q	quartz density (kg/m^3)

ACKNOWLEDGEMENTS

This work was performed under the auspices of the U.S. Department of Energy, Geothermal Technology Division. We thank S. Birdsell for reviewing this paper.

REFERENCES

Bohlman, E. G., Shor, A. J., Berlinski, P., and Mesmer, R. E., "Silica Scaling in Simulated Geothermal Brines," Oak Ridge National Laboratory Report No. TM-7681 (1981).

Brown, D. W., and Fehler, M. F., "The Pressure/Water-Loss Behavior of a Hydraulically Stimulated Region of Deep Naturally Jointed Crystalline Rock," presented at the 14th Workshop on Geothermal Reservoir Engineering, Stanford University, Stanford, CA (1989).

Cuellar, G., "Behavior of Silica in Geothermal Waste Waters," Second U.N. Symposium on the Development and Use of Geothermal Resources, San Francisco, CA (1975).

Gringarten, A. C., Witherspoon, P. A., and Ohnishi, Y., "Theory of Heat Extraction from Hot Dry Rock," J. Geophys. Res., 80, 1120-1124 (1975).

Gudmundsson, J. S., and Bott, T. R., "Deposition of Silica from Geothermal Waters on Heat Transfer Surfaces," Desalination, 28 (1979).

Horne, R. N., "Geothermal Reinjection Experience in Japan," Soc. Petrol. Eng. J., 495-503 (1982).

Makrides, A. C., et al., "Study of Silica Scaling From Geothermal Brines," U. S. Dept. of Energy Report Number COO-2607-5 (1978).

Marsh, A. R., Klein, G., and Vermeulen, T., "Polymerization Kinetics and Equilibria of Silicic Acid in Aqueous Systems," Laverence Berkeley Laboratory Report Number LBL-4415 (1975).

Rimstidt, J. D., and Barnes, H. L., "The Kinetics of Silica-Water Reactions," Geochim. et Cosmochim. Acta, 44, 1683-1699 (1980).

Robinson, B. A., "Quartz Dissolution and Silica Deposition in Hot Dry Rock Geothermal Systems," S. M. Thesis, MIT, Cambridge, MA (1982).

Rothbaum, H. P., and Anderton, B. H., "Removal of Silica and Arsenic from Geothermal Discharge Waters by Precipitation of Useful Calcium Silicates," Second U.N. Symposium on the Development and Use of Geothermal Resources, San Francisco, CA (1975).

Tester, J. W., Murphy, H. D., Grigsby, C. O., Potter, R. M., and Robinson, B. A., "Fractured Geothermal Energy Growth Induced By Heat Extraction," paper presented at the 56th SPE California Regional Meeting, Oakland, CA, SPE 15124, (1986).

White, D. E., Brannock, W. W., and Murata, K. J., "Silica in Hot-Spring Waters," Geochim. et Cosmochim. Acta, 10 (1956).